# New Decay Modes of the $\Lambda_c^+$ Charmed Baryon

R. Ammar,[1] P. Baringer,[1] A. Bean,[1] D. Besson,[1] D. Coppage,[1] N. Copty,[1] R. Davis,[1] N. Hancock,[1] M. Kelly,[1] S. Kotov,[1] I. Kravchenko,[1] N. Kwak,[1] H. Lam,[1] Y. Kubota,[2] M. Lattery,[2] M. Momayezi,[2] J. K. Nelson,[2] S. Patton,[2] R. Poling,[2] V. Savinov,[2] S. Schrenk,[2] R. Wang,[2] M. S. Alam,[3] I. J. Kim,[3] Z. Ling,[3] A. H. Mahmood,[3] J. J. O'Neill,[3] H. Severini,[3] C. R. Sun,[3] F. Wappler,[3] G. Crawford,[4] C. M. Daubenmier,[4] R. Fulton,[4] D. Fujino,[4] K. K. Gan,[4] K. Honscheid,[4] H. Kagan,[4] R. Kass,[4] J. Lee,[4] M. Sung,[4] C. White,[4] A. Wolf,[4] M. M. Zoeller,[4] F. Butler,[5] X. Fu,[5] B. Nemati,[5] W. R. Ross,[5] P. Skubic,[5] M. Wood,[5] M. Bishai,[6] J. Fast,[6] E. Gerndt,[6] J. W. Hinson,[6] R. L. McIlwain,[6] T. Miao,[6] D. H. Miller,[6] M. Modesitt,[6] D. Payne,[6] E. I. Shibata,[6] I. P. J. Shipsey,[6] P. N. Wang,[6] M. Battle,[7] J. Ernst,[7] L. Gibbons,[7] Y. Kwon,[7] S. Roberts,[7] E. H. Thorndike,[7] C. H. Wang,[7] J. Dominick,[8] M. Lambrecht,[8] S. Sanghera,[8] V. Shelkov,[8] T. Skwarnicki,[8] R. Stroynowski,[8] I. Volobouev,[8] G. Wei,[8] P. Zadorozhny,[8] M. Artuso,[9] M. Gao,[9] M. Goldberg,[9] D. He,[9] N. Horwitz,[9] G. C. Moneti,[9] R. Mountain,[9] F. Muheim,[9] Y. Mukhin,[9] S. Playfer,[9] Y. Rozen,[9] S. Stone,[9] X. Xing,[9] G. Zhu,[9] J. Bartelt,[10] S. E. Csorna,[10] Z. Egyed,[10] V. Jain,[10] D. Gibaut,[11] K. Kinoshita,[11] P. Pomianowski,[11] B. Barish,[12] M. Chadha,[12] S. Chan,[12] D. F. Cowen,[12] G. Eigen,[12] J. S. Miller,[12] C. O'Grady,[12] J. Urheim,[12] A. J. Weinstein,[12] M. Athanas,[13] W. Brower,[13] G. Masek,[13] H. P. Paar,[13] J. Gronberg,[14] C. M. Korte,[14] R. Kutschke,[14] S. Menary,[14] R. J. Morrison,[14] S. Nakanishi,[14] H. N. Nelson,[14] T. K. Nelson,[14] C. Qiao,[14] J. D. Richman,[14] A. Ryd,[14] D. Sperka,[14] H. Tajima,[14] M. S. Witherell,[14] R. Balest,[15] K. Cho,[15] W. T. Ford,[15] D. R. Johnson,[15] K. Lingel,[15] M. Lohner,[15] P. Rankin,[15] J. G. Smith,[15] J. P. Alexander,[16] C. Bebek,[16] K. Berkelman,[16] K. Bloom,[16] T. E. Browder,[16,*] D. G. Cassel,[16] H. A. Cho,[16] D. M. Coffman,[16] D. S. Crowcroft,[16] P. S. Drell,[16] D. J. Dumas,[16] R. Ehrlich,[16] P. Gaidarev,[16] M. Garcia-Sciveres,[16] B. Geiser,[16] B. Gittelman,[16] S. W. Gray,[16] D. L. Hartill,[16] B. K. Heltsley,[16] S. Henderson,[16] C. D. Jones,[16] S. L. Jones,[16] J. Kandaswamy,[16] N. Katayama,[16] P. C. Kim,[16] D. L. Kreinick,[16] G. S. Ludwig,[16] J. Masui,[16] J. Mevissen,[16] N. B. Mistry,[16] C. R. Ng,[16] E. Nordberg,[16] J. R. Patterson,[16] D. Peterson,[16] D. Riley,[16] S. Salman,[16] M. Sapper,[16] F. Würthwein,[16] P. Avery,[17] A. Freyberger,[17] J. Rodriguez,[17] S. Yang,[17] J. Yelton,[17] D. Cinabro,[18] T. Liu,[18] M. Saulnier,[18] R. Wilson,[18] H. Yamamoto,[18] T. Bergfeld,[19] B. I. Eisenstein,[19] G. Gollin,[19] B. Ong,[19] M. Palmer,[19] M. Selen,[19] J. J. Thaler,[19] K. W. Edwards,[20] M. Ogg,[20] A. Bellerive,[21] D. I. Britton,[21] E. R. F. Hyatt,[21] D. B. MacFarlane,[21] P. M. Patel,[21] B. Spaan,[21] and A. J. Sadoff[22]

(CLEO Collaboration)

[1]*University of Kansas, Lawrence, Kansas 66045*
[2]*University of Minnesota, Minneapolis, Minnesota 55455*
[3]*State University of New York at Albany, Albany, New York 12222*
[4]*The Ohio State University, Columbus, Ohio 43210*
[5]*University of Oklahoma, Norman, Oklahoma 73019*
[6]*Purdue University, West Lafayette, Indiana 47907*
[7]*University of Rochester, Rochester, New York 14627*
[8]*Southern Methodist University, Dallas, Texas 75275*
[9]*Syracuse University, Syracuse, New York 13244*
[10]*Vanderbilt University, Nashville, Tennessee 37235*
[11]*Virginia Polytechnic Institute and State University, Blacksburg, Virginia 24061*
[12]*California Institute of Technology, Pasadena, California 91125*
[13]*University of California, San Diego, La Jolla, California 92093*
[14]*University of California, Santa Barbara, California 93106*
[15]*University of Colorado, Boulder, Colorado 80309-0390*
[16]*Cornell University, Ithaca, New York 14853*
[17]*University of Florida, Gainesville, Florida 32611*
[18]*Harvard University, Cambridge, Massachusetts 02138*
[19]*University of Illinois, Champaign-Urbana, Illinois 61801*
[20]*Carleton University, Ottawa, Ontario, Canada K1S 5B6*
*and the Institute of Particle Physics, Montréal, Canada*
[21]*McGill University, Montréal, Québec, Canada H3A 2T8*
*and the Institute of Particle Physics, Montréal, Canada*
[22]*Ithaca College, Ithaca, New York 14850*
(Received 10 November 1994)

 0031-9007/95/74(18)/3534(4)$06.00 © 1995 The American Physical Society

We have observed five new decay modes of the charmed baryon $\Lambda_c^+$ using data collected with the CLEO II detector. Four decay modes, $\Lambda_c^+ \longrightarrow p\bar{K}^0\eta$, $\Lambda\eta\pi^+$, $\Sigma^+\eta$, and $\Sigma^{*+}\eta$, are first observations of final states with an $\eta$ meson, while the fifth mode, $\Lambda_c^+ \longrightarrow \Lambda\bar{K}^0K^+$, requires the creation of an $s\bar{s}$ quark pair. We measure the branching fractions of these modes relative to $\Lambda_c^+ \longrightarrow pK^-\pi^+$ to be $0.25 \pm 0.04 \pm 0.04$, $0.35 \pm 0.05 \pm 0.06$, $0.11 \pm 0.03 \pm 0.02$, $0.17 \pm 0.04 \pm 0.03$, and $0.12 \pm 0.02 \pm 0.02$, respectively.

PACS numbers: 13.30.Eg, 14.20.Lq

In the past year, CLEO has measured the exclusive decays of the $\Lambda_c^+$ into $\Lambda(n\pi)^+$, $\Sigma^0(n\pi)^+$, $\Sigma^+(n\pi)^0$, $pK^-(n\pi)^+$, and $pK_S^0(n\pi)^0$, where $n \leq 3$ and includes up to one $\pi^0$ [1–3]. In addition, CLEO has observed decays that are expected to occur solely through the $W$-exchange diagram (neglecting final state interactions), namely, $\Lambda_c^+ \longrightarrow \Sigma^+K^+K^-$, $\Xi^0K^+$, and $\Xi^-K^+\pi^+$ [4]. However, only ~35% of the $\Lambda_c^+$ hadronic decay modes have been accounted for [5]. Missing are higher multiplicity $\Lambda_c^+$ decay modes, especially those with multiple $\pi^0$'s, and modes with $\Sigma^-$ hyperons or neutrons in the final state, which are difficult to measure. Clearly, a substantial number of $\Lambda_c^+$ decay modes remain to be discovered.

This Letter presents results on five new $\Lambda_c^+$ decay modes. These include the first observation of four $\Lambda_c^+$ decay modes with an $\eta$ meson in the final state, namely, $\Lambda_c^+ \longrightarrow pK_S^0\eta$, $\Lambda\eta\pi^+$, $\Sigma^+\eta$, and $\Sigma^{*+}\eta$. The fifth mode is $\Lambda_c^+ \longrightarrow \Lambda K_S^0K^+$, which involves the creation of an $s\bar{s}$ quark pair. The decay modes discussed also include the charge conjugate states.

The data were collected with the CLEO II detector at the Cornell $e^+e^-$ storage ring CESR, which operated on and just below the $\Upsilon(4S)$ resonance. The CLEO II detector [6] is a large solenoidal detector with 67 tracking layers and a CsI electromagnetic calorimeter that provides excellent $\pi^0$ and $\eta$ reconstruction. We have used a total integrated luminosity of 3.25 fb$^{-1}$, which corresponds to $\sim 4 \times 10^6$ $c\bar{c}$ events.

The $\eta$ candidates are selected through the decay $\eta \longrightarrow \gamma\gamma$ from pairs of well-defined showers in the CsI calorimeter. To reduce random combinations of low energy photons, we require $E_\gamma > 0.15$ GeV for each photon candidate and $P_\eta > 0.5$ GeV/$c$. Photon candidates must not be associated with charged tracks and must have lateral shower shapes consistent with those expected for real photons. At least one of the photon candidates must lie in the barrel region defined by $|\cos\theta| < 0.71$, where $\theta$ is the polar angle with respect to the beam line. Photons are vetoed as $\eta$ daughters if they can be paired with a second photon such that the $\gamma\gamma$ pair has an invariant mass within $2.5\sigma$ of the $\pi^0$ mass ($\sigma \sim 5$ MeV/$c^2$) and a momentum greater than 0.4 GeV/$c$. We select $\eta$ candidates that are within 30 MeV/$c^2$ of the nominal $\eta$ mass. Finally, we kinematically fit the photon momenta to the nominal $\eta$ mass in order to improve the $\eta$ momentum estimate.

Charged proton, kaon, and pion candidates are required to have a specific ionization loss ($dE/dx$) and, when available, time-of-flight information consistent with the value expected for the assumed particle type. We use a clean sample of $\Lambda \longrightarrow p\pi^-$, $D^0 \longrightarrow K^-\pi^+$ from $D^{*+}$'s, and $K_S^0 \longrightarrow \pi^+\pi^-$ to measure the particle identification efficiencies directly from the data for protons, kaons, and pions, respectively.

The $K_S^0$ and $\Lambda$ candidates are selected through their decays $K_S^0 \longrightarrow \pi^+\pi^-$ and $\Lambda \longrightarrow p\pi^-$ by reconstructing a secondary decay vertex from the intersection of two oppositely charged tracks in the $r$-$\phi$ plane. The $\Sigma^+$ hyperon candidates are selected from $p\pi^0$ combinations that are consistent with coming from a decay vertex displaced from the primary interaction point [2]. The invariant masses of the $K_S^0$, $\Lambda$, and $\Sigma^+$ candidates must lie within 15, 5, and 15 MeV/$c^2$ of their nominal values, respectively.

Charmed baryons from $e^+e^- \longrightarrow c\bar{c}$ interactions are produced with a hard momentum spectrum, so we reduce the combinatoric background by requiring $x_p > 0.4$–$0.6$, depending on the decay mode. Here, $x_p = P_{\Lambda_c^+}/\sqrt{E_{\text{beam}}^2 - M_{\Lambda_c^+}^2}$ is the scaled momentum of the $\Lambda_c^+$. The $x_p$ cut eliminates $\Lambda_c^+$ baryons that arise from $B$ meson decays. In addition, we require that the daughter particles of the $\Lambda_c^+$ lie within 90 degrees of the candidate $\Lambda_c^+$ momentum vector.

The invariant mass distribution for $\Lambda_c^+ \longrightarrow pK_S^0\eta$ candidates with $x_p > 0.5$ is shown in Fig. 1. For this mode only, we tightened the particle identification criteria for the proton by requiring that the probability the candidate is a proton be at least 90% of the sum of probabilities for the proton, kaon, and pion hypotheses. We parametrize the mass distribution by a Gaussian signal and a third order Chebyshev polynomial background. The width of the Gaussian is taken from Monte Carlo studies to be $\sigma = 6.6$ MeV/$c^2$. We observe $57 \pm 10$ $\Lambda_c^+ \longrightarrow pK_S^0\eta$

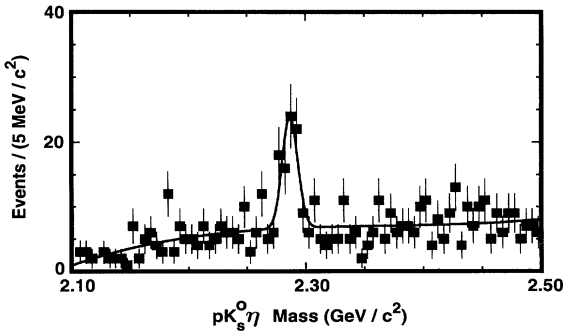


FIG. 1. Invariant mass distribution for $\Lambda_c^+ \longrightarrow pK_S^0\eta$.

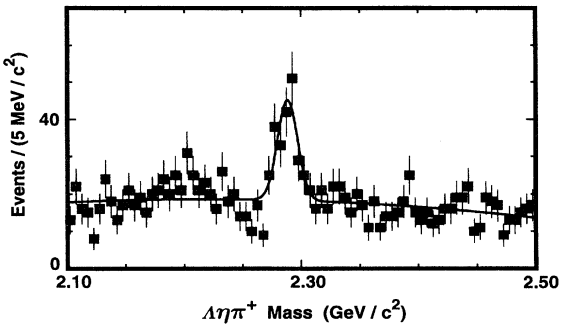


FIG. 2. Invariant mass distribution for $\Lambda_c^+ \longrightarrow \Lambda\eta\pi^+$.

events at a mass of 2286.7 ± 1.3 MeV/$c^2$ (statistical error only), consistent with the nominal $\Lambda_c^+$ mass.

The invariant mass distribution for $\Lambda_c^+ \longrightarrow \Lambda\eta\pi^+$ candidates with $x_p > 0.5$ is shown in Fig. 2. The signal is fit to a Gaussian whose width is fixed to the Monte Carlo expectation of 8.6 MeV/$c^2$; the background is parametrized by a quadratic polynomial. We observe 116 ± 16 events at a mass of 2288.5 ± 1.4 MeV/$c^2$.

A search was made for the two-body decay $\Lambda_c^+ \longrightarrow \Sigma^{*+}(1385)\eta$ by examining the resonant substructure of the $\Lambda\eta\pi^+$ mode. Figure 3 shows the invariant mass for $\Lambda\pi^+$ pairs in the $\Lambda_c^+ \longrightarrow \Lambda\eta\pi^+$ mass signal region ($\pm 2\sigma$) after subtracting combinations from the $\Lambda_c^+$ sideband region ($2.5 - 4.5\sigma$). A clear $\Sigma^{*+}$ peak is visible, which we fit to a Breit-Wigner distribution of width 36 MeV/$c^2$ plus the $\Lambda\pi^+$ mass distribution from the nonresonant decay of $\Lambda_c^+ \longrightarrow \Lambda\eta\pi^+$. The fit yields 54 ± 14 events at a mass of 1381 ± 5 MeV/$c^2$. This implies roughly half of the $\Lambda_c^+ \longrightarrow \Lambda\eta\pi^+$ decays are due to the two-body decay $\Lambda_c^+ \longrightarrow \Sigma^{*+}\eta$, neglecting any interference effects from other decay modes such as $\Lambda_c^+ \longrightarrow \Lambda a_0(980)$ where $a_0 \longrightarrow \eta\pi^+$. We searched for the $\Lambda a_0$ decay. However, because the $a_0$ width is quite large and not well measured (50–300 MeV/$c^2$) [5], we could not constrain the $\Lambda a_0$ decay component.

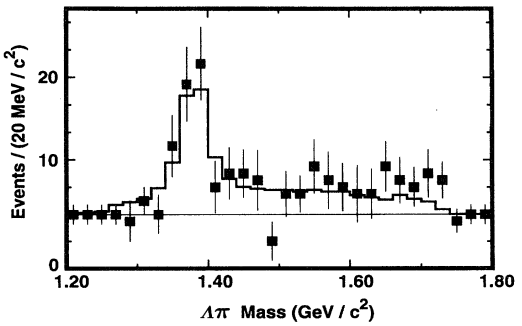


FIG. 3. The $\Lambda\pi^+$ invariant mass distribution for $\Lambda_c^+ \longrightarrow \Lambda\eta\pi^+$ candidates showing the $\Sigma^{*+}(1385)$ resonance. The points are data and the histogram is a fit to a Breit-Wigner signal and a phase space background, both of which include the effects of detector acceptance and resolution.

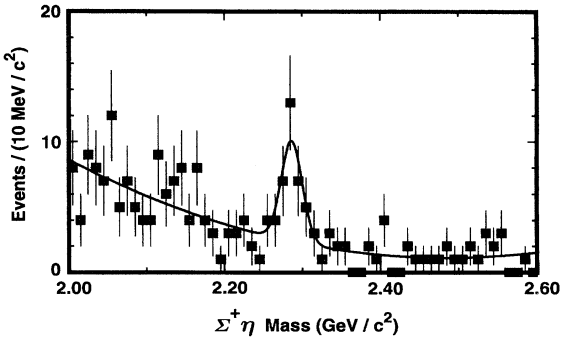


FIG. 4. Invariant mass distribution for $\Lambda_c^+ \longrightarrow \Sigma^+\eta$.

The invariant mass distribution for the two-body decay $\Lambda_c^+ \longrightarrow \Sigma^+\eta$ is shown in Fig. 4. We demand that the $\eta$, $\Sigma^+$, and $\Sigma^+\eta$ candidates have high momenta: $P_\eta > 0.8$ GeV/$c$, $P_{\Sigma^+} > 1.0$ GeV/$c$, and $x_p(\Lambda_c^+) > 0.6$, respectively. The $\pi^0$ veto on photons from $\eta$ mesons is not imposed because the combinatoric background for higher momenta $\eta$'s is less severe. The $\Sigma^+\eta$ mass distribution is fit to the sum of a Gaussian whose width is constrained to the Monte Carlo prediction of 13.6 MeV/$c^2$ and a quadratic background. We observe a $\Lambda_c^+ \longrightarrow \Sigma^+\eta$ signal of 26 ± 7 events at a mass of 2286 ± 4 MeV/$c^2$.

The $\Lambda_c^+ \longrightarrow \Lambda K_S^0 K^+$ invariant mass distribution is shown in Fig. 5. A less stringent $\Lambda_c^+$ momentum cut of $x_p > 0.4$ is used since the background level is low due to the clean $K_S^0$ and $\Lambda$ signals and the limited phase space available for this decay. The Gaussian width is fixed to the Monte Carlo expectation of 4.0 MeV/$c^2$ and a linear background is assumed. We observe a $\Lambda_c^+$ signal of 59 ± 9 events at a mass of 2286.5 ± 0.7 MeV/$c^2$. There is no indication of the resonant substructure $\Lambda_c^+ \longrightarrow \Lambda a_0(980)$ with $a_0$ decaying into $K_S^0 K^+$.

Since the $\Lambda_c^+$ cross section is unknown, we convert our observations into branching fractions relative to the well measured decay mode $\Lambda_c^+ \longrightarrow pK^-\pi^+$. For each mode we apply the same proton identification and $\Lambda_c^+$ momentum cut to the $\Lambda_c^+ \longrightarrow pK^-\pi^+$ sample in order to reduce the systematic errors associated with these re-

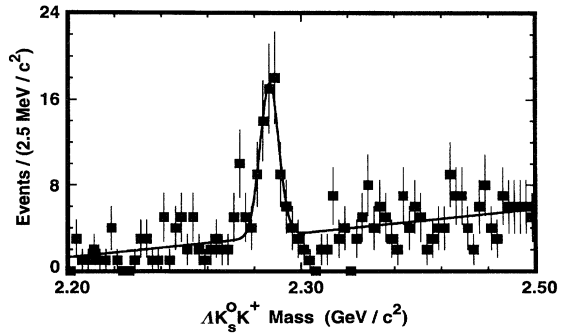


FIG. 5. Invariant mass distribution for $\Lambda_c^+ \longrightarrow \Lambda K_S^0 K^+$.

TABLE I. Summary of results on new $\Lambda_c^+$ decay modes. The efficiencies ($\mathcal{E}$) do not include branching fractions to the observed final states. The first error in the branching fraction is statistical and the second is systematic.

| Decay mode | Events | $\mathcal{E}$ (%) | $\mathcal{B}/\mathcal{B}(\Lambda_c^+ \to pK^-\pi^+)$ |
|---|---|---|---|
| $p\bar{K}^0\eta$ | $57 \pm 10$ | 7.2 | $0.25 \pm 0.04 \pm 0.04$ |
| $\Lambda\eta\pi^+$ | $116 \pm 16$ | 6.4 | $0.35 \pm 0.05 \pm 0.06$ |
| $\Sigma^+\eta$ | $26 \pm 7$ | 7.8 | $0.11 \pm 0.03 \pm 0.02$ |
| $\Sigma^{*+}\eta$ | $54 \pm 14$ | 6.8 | $0.17 \pm 0.04 \pm 0.03$ |
| $\Lambda\bar{K}^0K^+$ | $59 \pm 9$ | 8.9 | $0.12 \pm 0.02 \pm 0.02$ |

quirements. The raw yields, efficiencies, and resultant branching fractions for all decay modes are shown in Table I. The major contributions to the systematic errors are due to $K_S^0$, $\Lambda$, and $\Sigma^+$ reconstruction (5%–6%), $\eta$ reconstruction (5%), resonant substructure in the decay modes $\Lambda_c^+ \to pK^-\pi^+$ (2%–7%) and $\Lambda_c^+ \to \Lambda\eta\pi^+$ (10%), signal widths in the fits to the invariant mass distributions (4%–7%), and variations in the selection criteria (9%–15%). We have verified that backgrounds from misidentified $D^+$ and $D_s^+$ decays do not peak in the $\Lambda_c^+$ signal region. For example, the $pK_S^0\eta$ and $\Lambda\eta\pi^+$ invariant mass distributions show no contribution from possible misidentified $D^+ \to K_S^0\eta\pi^+$ decays.

The decay rates for the modes with an $\eta$ meson are about 2.0–2.5 times smaller than the related modes with a $\pi^0$, namely, the $\Lambda_c^+ \to p\bar{K}^0\pi^0$, $\Lambda\pi^+\pi^0$, and $\Sigma^+\pi^0$ decay modes, which are consistent with the light quark content of the $\eta$ being $\sim 1/3$ that of the $\pi^0$. (CLEO has measured [1–3] the branching fractions for $\Lambda_c^+ \to p\bar{K}^0\pi^0$, $\Lambda\pi^+\pi^0$, and $\Sigma^+\pi^0$ relative to $\Lambda_c^+ \to pK^-\pi^+$ to be $0.63 \pm 0.13$, $0.73 \pm 0.09 \pm 0.16$, and $0.20 \pm 0.03 \pm 0.03$, respectively.) In addition, the relative branching fraction for $\Lambda_c^+ \to \Lambda\bar{K}^0K^+$ is roughly 6 times smaller than the related decay mode without the $s\bar{s}$ pair creation, $\Lambda_c^+ \to \Lambda\pi^+\pi^0$.

The two-body decay modes $\Lambda_c^+ \to \Sigma^+\eta$ and $\Sigma^{*+}\eta$ are expected to proceed entirely through nonfactorizable internal $W$-emission and $W$-exchange diagrams. Unlike in charmed meson decays, these nonfactorizable decays are not color or helicity suppressed and contribute to the $\Lambda_c^+$ lifetime, being approximately half of the $D^0$ and $D_s^+$ meson lifetimes.

Körner and Krämer [7], Zenczykowski [8], and Uppal, Verma, and Khanna [9] have used quark and pole models to make theoretical predictions for the $\Lambda_c^+$ decays into two-body final states with $\Sigma^+$ and $\Sigma^{*+}$ hyperons. We have converted their decay rates into relative branching fractions, shown in Table II, using the Particle Data Group values for the $\Lambda_c^+$ lifetime and $\mathcal{B}(\Lambda_c^+ \to pK^-\pi^+)$ [5]. The high (low) value in Uppal's prediction includes (excludes) the effect of flavor dependence on the scale $|\psi(0)|^2$. The theoretical estimates agree with our results within a factor of 2. The ratio $\mathcal{B}(\Sigma^+\eta)/\mathcal{B}(\Sigma^+\pi^0)$ shows better agreement between theory and experiment.

In summary, we have observed five new decay modes of the charmed baryon $\Lambda_c^+$. Four decay modes, $\Lambda_c^+ \to p\bar{K}^0\eta$, $\Lambda\eta\pi^+$, $\Sigma^+\eta$, and $\Sigma^{*+}\eta$, contain an $\eta$ meson in the final state, while the fifth decay mode, $\Lambda_c^+ \to \Lambda\bar{K}^0K^+$, requires the creation of an $s\bar{s}$ quark pair. The branching fractions are measured relative to the decay mode $\Lambda_c^+ \to pK^-\pi^+$. Altogether, these new decay modes account for $\sim 4\%$ of all $\Lambda_c^+$ decays.

We gratefully acknowledge the effort of the CESR staff in providing us with excellent luminosity and running conditions. This work was supported by the National Science Foundation, the U.S. Department of Energy, the Heisenberg Foundation, the Alexander von Humboldt Stiftung, the SSC Fellowship program of TNRLC, the Natural Sciences and Engineering Research Council of Canada, and the A. P. Sloan Foundation.

*Permanent address: University of Hawaii at Manoa, Honolulu, HI 96801.

[1] CLEO Collaboration, P. Avery *et al.*, Phys. Lett. B **325**, 257 (1994).
[2] CLEO Collaboration, Y. Kubota *et al.*, Phys. Rev. Lett. **71**, 3255 (1993).
[3] CLEO Collaboration, D. Cinabro *et al.*, Report No. CLEO Conf 93-27, 1993.
[4] CLEO Collaboration, P. Avery *et al.*, Phys. Rev. Lett. **71**, 2391 (1993).
[5] Particle Data Group, L. Montanet *et al.*, Phys. Rev. D **50**, 1173 (1994).
[6] CLEO Collaboration, Y. Kubota *et al.*, Nucl. Phys. **A320**, 66 (1992).
[7] J. G. Körner and M. Krämer, Z. Phys. C **55**, 659 (1992).
[8] P. Zenczykowski, Phys. Rev. D **50**, 402 (1994).
[9] T. Uppal, R. C. Verma, and M. P. Khanna, Phys. Rev. D **49**, 3417 (1994).

TABLE II. Comparison of experimental branching fractions to theoretical predictions for the two-body decays $\Lambda_c^+ \to \Sigma^+\pi^0$, $\Sigma^+\eta$, and $\Sigma^{*+}\eta$ relative to $\Lambda_c^+ \to pK^-\pi^+$.

| | $\Sigma^+\pi^0$ [2] | $\Sigma^+\eta$ | $\Sigma^{*+}\eta$ |
|---|---|---|---|
| CLEO | $0.20 \pm 0.04$ | $0.11 \pm 0.04$ | $0.17 \pm 0.05$ |
| Körner and Krämer [7] | 0.07 | 0.04 | 0.24 |
| Zenczykowski [8] | 0.10 | 0.06 | ... |
| Uppal, Verma, and Khanna [9] | 0.13–0.58 | 0.05–0.24 | ... |